https://doi.org/10.5194/bg-2019-377
Preprint. Discussion started: 7 October 2019

Biogeosciences Discussions Open Access EGU

Phytoplankton productivity and rapid trophic transfer to microzooplankton stimulated by turbulent nitrate flux in oligotrophic Kuroshio Current

Toru Kobari[1*], Taiga Honma[2], Daisuke Hasegawa[3], Naoki Yoshie[4], Eisuke Tsutsumi[5], Takeshi Matsuno[6], Takeyoshi Nagai[7], Takeru Kanayama[2], Fukutaro Karu[2], Koji Suzuki[8], Takahiro Tanaka[3], Xinyu Guo[4], Gen Kume[1], Ayako Nishina[1] and Hirohiko Nakamura[1]

[1]Aquatic Sciences, Faculty of Fisheries, Kagoshima University
4-50-20 Shimoarata, Kagoshima, Kagoshima 890-0056, Japan
[2]Aquatic Sciences, Graduate School of Fisheries, Kagoshima University
4-50-20 Shimoarata, Kagoshima, Kagoshima 890-0056, Japan
[3]Tohoku National Fisheries Research Institute, Japan Fisheries Research and Education Agency
3-27-5 Shinhama-cho, Shiogama, Miyagi 985-0001, Japan
[4]Center for Marine Environmental Studies, Ehime University
2-5 Bunkyo-cho, Matsuyama, Ehime 790-8577, Japan
[5]Atmosphere and Ocean Research Institute, University of Tokyo
5-1-5 Kashiwanoha, Kashiwa, Chiba 277-8564, Japan
[6]Research Institute for Applied Mechanics, Kyushu University
6-1 Kasuga-koen, Kasuga, Fukuoka 816-8580, Japan
[7]Department of Ocean Sciences, Tokyo University of Marine Science and Technology
4-5-7 Konan Minato-ku, Tokyo 108-8477, Japan
[8]Faculty of Environmental Earth Science, Hokkaido University
North 10 West 5 Kita-ku, Sapporo, Hokkaido 060-0810, Japan

Correspondence to: Toru Kobari (kobari@fish.kagoshima-u.ac.jp)

https://doi.org/10.5194/bg-2019-377
Preprint. Discussion started: 7 October 2019

Biogeosciences Discussions Open Access EGU

Abstracts. The Kuroshio Current has been thought to be biologically unproductive due to oligotrophic conditions and low plankton standing stocks. Nevertheless, major foraging fishes are known to grow and recruit around the Kuroshio Current. While mixing and advection supplying nutrients to the euphotic zone are happened by eddies and meanders but limited at the Kuroshio front, there is a risk that survival of vulnerable life stages is encountered under the low food availability. Here we report that phytoplankton productivity is stimulated by turbulent nitrate flux amplified with the Kuroshio Current and rapidly transferred to microzooplankton through their grazing. Oceanographic observations demonstrate that the Kuroshio Current topographically enhances significant turbulent mixing and nitrate influx to the euphotic zone. Gradual nutrient enrichment experiments show growth rates of phytoplankton and microzooplankton communities stimulated within a range of the turbulent nitrate flux. Dilution experiments imply a significant microzooplankton grazing on phytoplankton. We propose that these rapid and systematic trophodynamics enhance invisible biological productivity in the Kuroshio.

https://doi.org/10.5194/bg-2019-377
Preprint. Discussion started: 7 October 2019

38 **1 Introduction**

39 The Kuroshio Current is the western boundary current of the North Pacific Subtropical Gyre (Qiu, 2001; Hu et
40 al., 2015). The upstream Kuroshio originates to the east of Taiwan, enters the East China Sea, and flows along the
41 continental slope until it passes through the Tokara Strait into the western North Pacific (Fig 1a). The Kuroshio has been
42 thought to be biologically unproductive because ambient nutrient concentrations and plankton standing stocks in its waters
43 are low (Guo, 1991; Hirota, 1995). In spite of such unproductive conditions, the Kuroshio in the East China Sea (ECS-
44 Kuroshio) is neighboring major spawning and nursery grounds for foraging species such as sardine (Watanabe et al.,
45 1996), jack mackerel (Sassa et al., 2008), and chub mackerel (Sassa and Tsukamoto, 2010), and common squid (Bower
46 et al., 1999). It seems unlikely that highly vulnerable early life stages of many foraging species would successfully grow
47 and recruit neighboring the oligotrophic and unproductive waters around the ECS-Kuroshio (hereafter called the
48 “Kuroshio Paradox”: Saito, 2019), even if the warm temperatures of the Kuroshio Current could enhance cellular
49 metabolic processes and then growth. It has been believed that survival of these early stages is supported by high plankton
50 productivity on the continental shelf and in the Kuroshio front (Nakata et al., 1995). However, such good food availability
51 is spatially limited and greatly variable because the Kuroshio Current often meanders (Nakata and Hidaka, 2003).
52 Otherwise, the coastal water mass is sometimes entrapped and transported into the Kuroshio and more pelagic sites
53 (Nakamura et al., 2006; Kobari et al., 2019). Use of waters in the vicinity of the oligotrophic Kuroshio as a nursery and
54 feeding ground would therefore appear to be a risky strategy unless there is a mechanism that enhance biological
55 production in the Kuroshio.

56 Here we report phytoplankton productivity stimulated by turbulent nitrate flux that can happen in the Kuroshio
57 Current and its rapid trophic transfer to microzooplankton through their extensive grazing. Oceanographic observations

https://doi.org/10.5194/bg-2019-377
Preprint. Discussion started: 7 October 2019

demonstrate a significant nitrate flux caused by turbulent mixing in the Tokara Strait of the ECS-Kuroshio. Nutrient-amended bottle incubation experiments show phytoplankton and microzooplankton growths elevated within a range of this turbulent nitrate flux and significant grazing of microzooplankton on phytoplankton.

2 Materials and methods

2.1 Onboard observations and experiments

All oceanographic observations and bottle incubations were done in the Kuroshio Current where it passes through the Tokara Strait. Sampling for nitrate concentrations and measurements of turbulent diffusivity were conducted at 14 stations along the 2 lines across the Kuroshio Current (Fig 1a) during cruises of the T/S *Kagoshima-maru* in November 2015.

We measured turbulent diffusivity and nitrate concentrations using a turbulent microstructure profiler (TurboMAP-L; JFE Advantech Co. Ltd.) and an *in situ* nitrate sensor (DEEP SUNA V2; Sea-Bird Scientific), respectively. Both parameters were binned and averaged within 10-meter intervals. The vertical gradient of the averaged nitrate profile (C_{NO3}) and the averaged vertical diffusivity profile (K_z) were then multiplied at each depth (z) to estimate the area-averaged vertical turbulent nitrate flux (F_{NO3}) with the following equation:

$$F_{NO3} = -K_Z \times \partial C_{NO3} / \partial z \quad (1)$$

Bottle incubations were performed for phytoplankton and microzooplankton growth rates in response to nutrient gradient (EXP_a) at 8 stations in November 2016 and 2017 and for microzooplankton grazing (EXP_b) at 8 stations in November 2017 (Fig 1b, Table 1).

https://doi.org/10.5194/bg-2019-377
Preprint. Discussion started: 7 October 2019

78 **2.2 Experimental setup**

79 Seawater samples for all experiments were obtained using 2.5-L Niskin-X bottles attached to a conductivity-
80 temperature-depth profiler and carousel multisampling system (CTD-CMS: Sea−Bird SBE-9plus). The samples were
81 transferred by gravity filtration using a silicon tube with a nylon filter (0.1-mm mesh opening) into the incubation bottles
82 for EXP_a and EXP_b. EXP_a was performed using duplicate 2.3-L polycarbonate bottles without added nutrients and with a
83 mixture of nitrate ($NaNO_3$) and phosphate (KH_2PO_4) in an atomic N:P ratio of 15:1. The nitrate concentrations were either
84 0 (control), 0.05, 0.15, 0.5, 0.75, 1.5, or 5 μmol L^{-1}. Assuming that the turbulent nitrate supplies at the subsurface
85 chlorophyll maximum observed in the Tokara Strait (*O*: 0.788 mmol m^{-2} d^{-1}, see Results) was continued during 5.3 days
86 when the Kuroshio Current (0.33 m s^{-1}, Zhu et al., 2017) pass over the Tokara Strait (150 km) and consumed by
87 phytoplankton in a 10-m thick layer, it was equivalent to the nitrate enrichment of 0.41 μmol L^{-1}. The dilution experiments
88 (Landry and Hasset, 1982) (EXP_b) were conducted using triplicate 1.2-L polycarbonate bottles with microzooplankton as
89 grazers and involved four dilution factors (10, 30, 60, and 100%) of the microzooplankton standing stocks in the original
90 water samples. These treatment bottles were enriched with 3 μmol L^{-1} nitrate ($NaNO_3$) and 0.2 μmol L^{-1} phosphate
91 (KH_2PO_4) to promote phytoplankton growth. For evaluating nutrient limitation on phytoplankton growth, no enrichment
92 was conducted for triplicate non-diluted bottles (100%). All incubation tools were soaked in 10% HCl and rinsed with
93 surface seawater at each station before use (Landry et al., 1995). All experimental bottles were incubated for 72 h for
94 EXP_a and 24 h for EXP_b in a water bath with running surface seawater for temperature control and covered by a nylon
95 mesh screening (5-mm mesh opening screening to reduce irradiance to 50% of the surface irradiance. Note that the
96 phytoplankton growth in the incubation bottles might be overestimated due to the weaker irradiance at subsurface than
97 those under the incubation conditions.

https://doi.org/10.5194/bg-2019-377
Preprint. Discussion started: 7 October 2019

98

99 **2.3 Sample analysis**

100 Chlorophyll *a* concentrations were determined at the beginning and end of the incubations for EXP_a and EXP_b.
101 Subsamples of 500 to 1000 mL were filtered through a nylon mesh (11-µm mesh opening: Millipore NY1104700) and a
102 glass-fiber filter (2-µm: Whatman GM/F, 0.7-µm: Whatman GF/F) for EXP_a and through a glass-fiber filter (GF/F) for
103 EXP_b at a pressure less than 20 kPa. Photosynthetic pigments were extracted overnight in *N,N*−dimethylformamide at –
104 20°C in the dark, and the chlorophyll *a* concentrations were determined with a fluorometer (Turner Designs 10AU or
105 TD700).

106 Microzooplankton in the incubation bottles at the beginning of EXP_a and EXP_b were examined. Subsamples of
107 500 mL were collected and fixed with 3% acid Lugol's solution. We identified and counted three taxonomic groups of
108 the microzooplankton community with an inverted microscope (Leica Leitz DMRD). Some marine planktonic ciliates
109 and flagellates are known to be mixotrophs (Gaines and Elbrächter, 1987), but we assumed naked ciliates and tintinnids
110 to be heterotrophic in the present study. The sizes of cells or individuals were measured, biovolume was computed based
111 on geometric shape, and the carbon content was estimated using conversion equations (Put and Stoecker, 1989; Verity
112 and Langdon, 1984; Parsons et al., 1984).

113

114 **2.4 Rate calculation**

115 Growth rates (g: d^{-1}) in the incubation bottles of EXP_a and EXP_b were calculated from size-fractionated
116 chlorophyll *a* concentrations (µg L^{-1}) or standing stocks (µgC L^{-1}) of microzooplankton groups identified at the beginning
117 (C_o) and end (C_t) of the incubations period (t: days):

118 $$G = [\ln(C_t) - \ln(C_o)]/t \quad (2)$$

https://doi.org/10.5194/bg-2019-377
Preprint. Discussion started: 7 October 2019

Apparent growth rates in the incubation bottles of EXP_b were calculated using the following model (Landry et al., 1995):

$$C_t = C_o \times \exp[(g_{max} - m) \times t] \quad (3)$$

where g_{max} and m are the maximum growth rate of size-fractionated phytoplankton (d^{-1}) and their mortality rate by microzooplankton grazing (d^{-1}), respectively. The maximum growth rate and mortality rate were determined with a linear regression of the apparent growth rate against dilution factors (X):

$$g = g_{max} - mX \quad (4)$$

All parameters derived from EXP_a and EXP_b are listed in Table 2 and Table 3.

3 Results

3.1 Oceanographic observations

First, turbulent diffusivity and nitrate concentrations were measured in order to estimate the vertical turbulent nitrate flux along the transects across the Kuroshio Current in the Tokara Strait, where a shallow ridge lies in the Kuroshio's path. We obtained 16 pairs of vertical profiles and estimated the averages and 95 percent confidence intervals. The averaged chlorophyll-*a* profile (Fig 2a) recorded with a light-emitting diode fluorometer on a TurboMAP-L profiler revealed a subsurface chlorophyll maximum (SCM) at 60 m, which was almost coincident with a sharp increase in the nitrate concentration (i.e., the top of the nitracline). Vertical diffusivity of O (10^{-4} m^2 s^{-1}, Fig 2b) was higher at 70 m compared with those in the layers between 80 and 130 m. Just below the SCM peak, relatively high nitrate concentrations and vertical diffusivity induced vertical turbulent nitrate fluxes of O (1 mmol m^{-2} d^{-1}, Fig 2c).

3.2 Gradient enrichment experiments (EXP_a)

To evaluate the effect of these turbulent nitrate fluxes measured in the Tokara Strait on the standing stocks of

https://doi.org/10.5194/bg-2019-377
Preprint. Discussion started: 7 October 2019

140 phytoplankton and microzooplankton in the Kuroshio, we conducted bottle incubations of the phytoplankton and
141 microzooplankton communities enriched with the different nutrient concentrations (EXP_a). The total chlorophyll *a*
142 concentrations at the beginning of the EXP_a averaged among the duplicate samples ranged from 0.15 to 0.52 μg L^{-1} (Table
143 1). The pico-fractions defined as smaller than 2 μm and nano-fractions between 2 to 11 μm accounted for more than 80%
144 of the total chlorophyll *a* (Fig 3a). All size-fractionated chlorophyll *a* declined or changed little toward the end of the
145 incubations at the nitrate enrichments below 0.15 μmol L^{-1}, but they increased at the enrichments above 0.5 μmol L^{-1}. At
146 the beginning of the incubations, microzooplankton standing stocks averaged among the duplicate samples ranged from
147 0.12 to 0.79 μg C L^{-1} (Table 1). Naked ciliates accounted for 51 to 96% of the microzooplankton community in terms of
148 carbon at the beginning of the incubations. Copepod nauplii were the second contributor to the microzooplankton
149 community due to the low abundance and large individual body mass, and tintinnid ciliates were a minor component. The
150 standing stocks of all taxonomic groups in the microzooplankton community increased with the higher nitrate enrichments
151 (Fig 3b), but the increasing patterns to nutrient gradient were less clear than those of the size-fractionated chlorophyll *a*
152 concentrations.

153 Based on these differences of the standing stocks between the beginning and end of the incubations, we
154 investigated the growth rates of chlorophyll and microzooplankton. The growth rates of all size-fractionated chlorophyll
155 increased at the larger nitrate additions (Fig 4a). Growth rates were negative or close to zero for all size-fractions at the
156 enrichment below 0.15 μmol L^{-1}. However, the pico- and micro-sized chlorophyll revealed positive growth rates at the
157 nitrate concentrations above 0.5 μmol L^{-1}, which were nearly equivalent to the turbulent nitrate fluxes observed in the
158 Tokara Strait (see Experimental setup). Because microzooplankton growth rates varied among stations, the response of
159 microzooplankton growth to nutrient gradient was ambiguous (Fig 4b). Growth rates were positive for copepod nauplii

https://doi.org/10.5194/bg-2019-377
Preprint. Discussion started: 7 October 2019

at all nitrate enrichments and were higher for both naked and tintinnid ciliates at the larger nitrate enrichments.

The slope of a linear regression between growth rates of the size-fractionated chlorophyll and the logarithms of the nitrate enrichments at each incubation provided a metric of the sensitivity of their growth rates to nutrient supply (Supplement Fig 1). To explain why growth rates of the size-fractionated chlorophyll varied among stations, the slopes were compared to the nitrate+nitrite (Fig 5a) and phosphate concentrations (Fig 5b) at the start of the incubations. There was a negative correlation of the slopes for all size-fractionated chlorophyll to the nitrate plus nitrite or phosphate concentrations, indicating that the stimulation of their growth rates by nutrients supply was greater for all size-fractionated chlorophyll under more oligotrophic conditions.

3.3 Dilution experiments (EXP_b)

The dilution experiments determined how and which the size-fractionated chlorophyll was removed by microzooplankton grazing. The maximum growth rates represented by the intercepts in the dilution experiments were relatively high for the nano-sized chlorophyll (Fig 6a), while the difference was insignificant among the three size-fractions (ANOVA, $p>0.05$). These findings indicated that growth potential under no microzooplankton grazing was slightly high for the nano-sized chlorophyll compared with those for the pico- and micro-fractions. On the other hand, the slopes were representative of the mortality rates by microzooplankton grazing and significantly higher for the nano-sized chlorophyll than those for the pico- and micro-sized chlorophyll (ANOVA+Tukey, $p<0.05$), indicating the preference of microzooplankton grazing on the nano-sized chlorophyll. To evaluate the impact of microzooplankton grazing on phytoplankton growth, we compared the three different net growth rates, which were the observed net growth rates without enrichment (g_o) and with enrichment (g_{en}) in the non-diluted bottles and the estimated net growth rates (g_{en}')

https://doi.org/10.5194/bg-2019-377
Preprint. Discussion started: 7 October 2019

subtracted the mortality rates (m) from the maximum growth rates (g_{max}). All size-fractionated chlorophyll demonstrated g_o lower than g_{en} (Fig 7), indicating nutrient limitation on the net growth rates. Both g_{en} an g_{en}' were comparable due to no significant difference between the two (Welch's *t*-test). These results imply that g_{en} of all size-fractionated chlorophyll balances the microzooplankton grazing mortality with the maximum growth. Particularly for the nano-fractionated chlorophyll, the net growth rates were slightly low due to the mortality rates by microzooplankton grazing exceeded the maximum growth rates.

4 Discussion

The Kuroshio Current impinges on numerous shallow ridges with small islands and seamounts in the Tokara Strait. Several studies have pointed out that those steep topographic features stir and modify the water column through upwelling (Hasegawa et al., 2004, 2008) and turbulent mixing (Tsutsumi et al., 2017; Nagai et al., 2017). Comparing with the turbulent nitrate fluxes among the previously study sites, the fluxes observed in the Tokara Strait of the Kuroshio Current were one order higher than those reported in the Kuroshio Extension front (Kaneko et al., 2012, 2013; Nagai et al., 2017), much greater than those at other oceanic sites, and equivalent to those at coastal sites (Cyr et al., 2015). The turbulent nitrate flux in the downstream Kuroshio Current where was close to the Tokara Strait was similar magnitude to our estimates (Nagai et al., 2019). Since the Kuroshio Current steadily runs in the Tokara Strait, such nutrient supply induced by turbulence diffusivity is considered as one of mechanisms that phytoplankton productivity is enhanced even under oligotrophic Kuroshio.

In spite of the large turbulent nitrate flux (*O*: 1 mmol m^{-2} d^{-1}), the chlorophyll *a* concentrations in the Tokara Strait of the Kuroshio Current were as low as the values reported from the neighboring Kuroshio (Kobari et al., 2018,

https://doi.org/10.5194/bg-2019-377
Preprint. Discussion started: 7 October 2019

2019) and oceanic sites in the North Pacific Ocean (Calbet and Landry, 2004). Based on the gradient enrichment experiments, standing stocks and their growth rates of all size-fractionated phytoplankton increased at the nitrate enrichments above 0.5 μmol L^{-1} that were equivalent to the observed turbulent nitrate flux. These results suggest that phytoplankton standing stocks and growths are stimulated by the magnitude of the observed turbulent nitrate flux. In the global comparisons, microzooplankton reveal a significant grazing impact on phytoplankton, particularly in oceanic sites (Calbet and Landry, 2004). Microzooplankton standing stocks in the Kuroshio Current at the Tokara Strait were lower than those on the continental shelf of the ECS (Chen et al., 2003), expecting low microzooplankton grazing on phytoplankton. However, the dilution experiments demonstrated that phytoplankton mortality by microzooplankton grazing was significantly high and equivalent to 41 to 122% of maximum growth rates of phytoplankton based on the ratio of the mortality rate to the maximum growth rates for total chlorophyll *a* (Table 2). Indeed, phytoplankton net growth likely balances microzooplankton grazing mortality with phytoplankton maximum growth, particularly for nano-fractionated phytoplankton. These results from the simultaneously conducted experiments suggest that phytoplankton standing stocks are stimulated by turbulent nitrate flux and then quickly removed by microzooplankton grazing, particularly for nanophytoplankton. Taking into account for the size range of prey for ciliates (Pierce and Turner, 1992) and copepod nauplii (Uye and Kasahara, 1983), microzooplankton grazing would be a major reason why phytoplankton do not attain high growth rates and standing stocks, even under the high potential growth and sensitive to nutrient enrichments. Thereby, the rapid transfer of the elevated phytoplankton production to microzooplankton might be a possible mechanism of the low chlorophyll even under the large turbulent nitrate flux in the Kuroshio Current.

The standing stocks and growth rates of all microzooplankton groups were relatively higher at the larger nitrate enrichments, but the increasing patterns were less clear than those of phytoplankton. This difference was probably due to

https://doi.org/10.5194/bg-2019-377
Preprint. Discussion started: 7 October 2019

the large variations in microzooplankton standing stocks among stations and slower growth than phytoplankton. Indeed, such unclear pattern was remarkable for copepod nauplii representing their slower growth rate, less abundance in the bottle and large individual body mass. More importantly, the results from the simultaneously conducted experiments imply that phytoplankton productivity is stimulated by the turbulent nitrate flux and rapidly transferred to microzooplankton through their extensive grazing but microzooplankton standing stocks and growths are not elevated during 3 days in the Kuroshio Current. Such elevated microzooplankton standing stocks and their trophic transfer to mesozooplankton might be found in the further downstream of the Kuroshio Current.

There is increasing information that turbulence-induced nutrient fluxes have been suggested to promote phytoplankton growth in the open ocean (Kaneko et al., 2013; Nagai et al., 2017, 2019), however, no experimental documentation is available for response of phytoplankton community to the nutrient supply or of subsequent trophic transfer in a planktonic food web. In the tropical and subtropical oceans, microzooplankton grazing has been thought to be a major source of phytoplankton mortality and has been shown to account for more than 75% of phytoplankton daily growth (Calbet and Landry, 2004). Furthermore, strong trophic linkages are well known between microbes and metazoans through microzooplankton (Calbet and Landry, 1999; Calbet et al., 2001; Calbet and Saiz, 2005; Kobari et al., 2010). Our study has provided the first experimental evidence that phytoplankton standing stocks and growths are stimulated by turbulent nutrient fluxes and rapidly transferred to microzooplankton via their grazing. These results imply a possibility that biological productivity is underestimated by apparent low nutrients and low phytoplankton biomass in the Kuroshio. Because strong turbulence amplified by the Kuroshio Current, phytoplankton productivity stimulated by the nutrient flux and rapid trophic transfer to microzooplankton are likely happened in the Tokara Strait and the downstream, we propose that invisible biological productivity in the Kuroshio is sustained by these rapid and systematic trophodynamics. Such

https://doi.org/10.5194/bg-2019-377
Preprint. Discussion started: 7 October 2019

240 invisible biological production elevated by the rapid and systematic trophodynamics may provide good food availability
241 for the vulnerable stages of foraging fishes around the Kuroshio and thus explain a part of the Kuroshio Paradox.
242
243 **Data Availability Statement:**
244 All relevant data are shown in the paper as tables and figure.
245
246 **Author Contributions**
247 T. Kobari, DH and NY conceived and designed the oceanographic observations and experiments. DH, HN, AN,
248 ET, TM, TN performed the oceanographic observations and turbulence measurements. T. Kobari, TH, T. Kanayama and
249 FK performed the onboard experiments. T. Kobari, TH, T. Kanayama, FK, NY, KS analyzed the samples and data of the
250 onboard experiments. DH and TT analyzed the data of oceanographic observations and turbulence measurements. T.
251 Kobari, GK, HN and XG organized the research cruises.
252
253 **Competing interests:**
254 The authors declare no competing and conflict interests.
255
256 **Acknowledgements**
257 We thank the captains and crew of the T/S *Kagoshima Maru* for their help in oceanographic observations and
258 sample collections.
259

https://doi.org/10.5194/bg-2019-377
Preprint. Discussion started: 7 October 2019

Financial support:

This study has been supported by grants from the Japan Society for the Promotion of Science (17K00522, 18H04920, 4702), Ministry of Education, Culture, Sports, Science and Technology in Japan (The Study of Kuroshio Ecosystem Dynamics for Sustainable Fisheries).

References

Bower, J.R., Nakamura, Y., Mori, K., Yamamoto, J., Isoda, Y., Sakurai, Y.: Distribution of *Todarodes pacificus* (Cephalopoda: Ommastrephidae) paralarvae near the Kuroshio off southern Kyushu, Japan, Mar. Biol., 135, 99–106, 1999.

Calbet, A., Landry, M. R.: Mesozooplankton influences on the microbial food web: Direct and indirect trophic interactions in the oligotrophic open-ocean, Limnol. Oceanogr., 44, 1370–1380, 1999.

Calbet, A., Landry, M. R.: Nunnery S. Bacteria-flagellate interactions in the microbial food web of the oligotrophic subtropical North Pacific, Aquat. Microb. Ecol., 23, 283–292, 2001.

Calbet, A., Landry, M. R.: Phytoplankton growth, microzooplankton grazing, and carbon cycling in marine systems. Limnol. Oceanogr., 49, 51–57, 2004.

Calbet, A., Saiz, E.: The ciliate-copepod link in marine ecosystems, Aquat. Microb. Ecol., 38, 157–167, 2005.

Chen, C.C., Shiah, F.K., Gong, G.C., Chiang, K.P.: Planktonic community respiration in the East China Sea: importance of microbial consumption of organic carbon. Deep-Sea Res. II, 50, 1311–1325, 2003.

Cyr, F., Bourgault, D., Galbraith, P. S.: Gosselin M. Turbulent nitrate fluxes in the Lower St. Lawrence Estuary, Canada. J. Geophys. Res., 120, 2308–2330, 2015.

Gaines, G., Elbrächter. M.: Heterotrophic nutrition, in The biology of dinoflagellates, edited by: Taylor, F. J. R., Blackwell,

https://doi.org/10.5194/bg-2019-377
Preprint. Discussion started: 7 October 2019

281 Oxford, 224–268, 1987.

282 Guo, Y. J.: The Kuroshio, Part II. Primary production and phytoplankton, Oceanogr. Mar. Bio. Ann. Rev., 29, 155–189,

283 1991.

284 Hasegawa, D., Yamazaki, H., Ishimaru, T., Nagashima, H., Koike, Y.: Apparent phytoplankton bloom due to island mass

285 effect, J. Mar. Syst., 69, 238–246, 2008.

286 Hasegawa, D., Yamazaki, H., Lueck, R. G., Seuront, L.: How islands stir and fertilize the upper ocean, Geophys. Res.

287 Lett., 31, L16303, 2004.

288 Hirota, Y.: The Kuroshio, Part III. Zooplankton, Oceanogr Mar. Bio. Ann. Rev., 33, 151–220, 1995.

289 Hu, D., Wu, L., Cai, W., Gupta, A. S., Ganachaud, A., Qiu, B., Gordon, A. L., Lin, X., Chen, Z., Hu, S., Wang, G.,

290 Wang, Q., Sprintall, J., Qu, T., Kashino, Y., Wang, F., William S. Kessler, W. S.: Pacific western boundary

291 currents and their roles in climate, Nature, 522, 299–308, 2015.

292 Kaneko, H., Yasuda, I., Komatsu, K., Itoh, S.: Observations of the structure of turbulent mixing across the Kuroshio,

293 Geophys. Res. Lett., 39, L15602, 2012.

294 Kaneko, H., Yasuda, I., Komatsu, K., Itoh, S.: Observations of vertical turbulent nitrate flux across the Kuroshio, Geophys.

295 Res. Lett., 40, 3123–3127, 2013.

296 Kobari, T., Kobari, Y., Miyamoto, H., Okazaki, Y., Kume, G., Kondo, R., Habano, A.: Variability in taxonomic

297 composition, standing stock and productivity of the plankton community in the Kuroshio and its neighboring

298 waters, in: Kuroshio Current, Physical, Biogeochemical and Ecosystem Dynamics, edited by: Nagai, T., Saito,

299 H., Suzuki, K., Takahashi, M., Geophysical Monograph 243, John Wiley & Sons, Hoboken, 223–350, 2019.

300 Kobari, T., Makihara, W., Kawafuchi, T., Sato, K., Kume, G.: Geographic variability in taxonomic composition, standing

https://doi.org/10.5194/bg-2019-377
Preprint. Discussion started: 7 October 2019

301 stock, and productivity of the mesozooplankton community around the Kuroshio Current in the East China Sea,
302 Fish. Oceanogr., 27, 336–350, 2018.
303 Kobari, T., Mitsui, K., Ota, T., Ichinomiya, M., Gomi, Y.: Response of heterotrophic bacteria to the spring phytoplankton
304 bloom in the Oyashio region. Deep-Sea Res. II., 57, 1671–1678, 2010.
305 Landry, M. R., Hasset, R. P.: Estimating the grazing impact of marine micro-zooplankton, Mar. Biol., 67, 283–288,
306 1982.
307 Landry, M. R., Kirshtein, J., Constantinou, J.: A refined dilution technique for measuring the community grazing impact
308 of microzooplankton with experimental tests in the central equatorial Pacific, Mar. Ecol. Prog. Ser., 120, 53–63,
309 1995.
310 Nagai, T., Clayton, S.: Nutrient interleaving below the mixed layer of the Kuroshio Extension front. Ocean Dyn., 67,
311 1027–1046, 2017.
312 Nagai, T., Durán, G. S., Otero, D. A., Mori, Y., Yoshie, N., Ohgi, K., Hasegawa, D., Nishina, A., Kobari, T.: How the
313 Kuroshio Current delivers nutrients to sunlit layers on the continental shelves with aid of near-internal waves
314 and turbulence, Geophys. Res. Lett., 46, 10.1029/2019GL082680, 2019.
315 Nagai, T., Hasegawa, D., Tanaka, T., Nakamura, H., Tsutsumi, E., Inoue, R., Yamashiro, T.: First evidence of coherent
316 bands of strong turbulent layers associated with high-wavenumber internal-wave shear in the upstream Kuroshio,
317 Sci. Rep., 7, 14555, 2017.
318 Nakamura, H., Yamashiro, T., Nishina, A., Ichikawa, H.: Time frequency variability of Kuroshio meanders in Tokara
319 Strait, Geophys. Res. Lett., 33, L21605, 2006.
320 Nakata, K., Hidaka, K.: Decadal-scale variability in the Kuroshio marine ecosystem in winter, Fish. Oceanogr., 12, 234–

https://doi.org/10.5194/bg-2019-377
Preprint. Discussion started: 7 October 2019

244, 2003.

Nakata, K., Zenitani, H., Inagake, D.: Differences in food availability for Japanese sardine larvae between the frontal region and the waters on the offshore side of Kuroshio, Fish. Oceanogr., 4, 68–79, 1995.

Parsons, T. R., Takahashi, M., Hargrave, B.: Biological oceanographic processes, Pergamon Press, Oxford, 1984.

Pierce, R. W., Turner, J. T.: Ecology of planktonic ciliates in marine food webs, Rev. Aquat. Sci., 6, 139–181, 1992.

Putt, M., Stoecker, D. K.: An experimentally determined carbon:volume ration for marine "oligotrichous" ciliates from estuarine and coastal waters, Limnol. Oceanogr., 34, 1097–1103, 1989.

Qiu, B.: Kuroshio and Oyashio Currents, in: Encyclopedia of Ocean Sciences, edited by: Steele, J. H., Academic Press, New York, 358–369, 2001.

Saito, H.: The Kuroshio: its recognition, scientific activities and emerging issues, in: Kuroshio Current, Physical, Biogeochemical and Ecosystem Dynamics, edited by: Nagai, T., Saito, H., Suzuki, K., Takahashi, M., Geophysical Monograph 243, John Wiley & Sons, Hoboken, 1–11, 2019.

Sassa, C., Tsukamoto, Y.: Distribution and growth of *Scomber japonicus* and *S. australasicus* larvae in the southern East China Sea in response to oceanographic conditions, Mar. Ecol. Prog. Ser., 419, 185–199, 2010.

Sassa, C., Tsukamoto, Y., Nishiuchi, K., Konishi, Y.: Spawning ground and larval transport processes of jack mackerel *Tranchurus japonicas* in the shelf-break region of the southern East China Sea, Cont. Shelf. Res., 28, 2574–2583, 2008.

Tsutsumi, E., Matsuno, T., Lien, R. C., Nakamura, H., Senjyu, T., Guo, X.: Turbulent mixing within the Kuroshio in the Tokara Strait, J. Geophys. Res. Oceans, 122, 10.1002/2017JC013049, 2017.

Uye, S. I., Kasahara, S,: Grazing of various developmental stages of *Pseudodiaptomus marinus* (Copepoda: Calanoida)

https://doi.org/10.5194/bg-2019-377
Preprint. Discussion started: 7 October 2019

on naturally occurring particles, Bull. Plankton Soc. Japan, 30, 147–158, 1983.

Verity, P.G., Langdon, C.: Relationships between lorica volume, carbon, nitrogen and ATP content of tintinnids in Narragansett Bay, J. Plankton Res., 6, 859–868, 1984.

Watanabe, Y., Zenitani, H., Kimura, R.: Offshore expansion of spawning of the Japanese sardine, *Sardinops melanostictus*, and its implication for egg and larval survival, Can. J. Fish. Aquat. Sci., 53, 55–61, 1996.

Zhu, X. H., Nakamura, H., Dong, M., Nishina, A., Yamashiro, T.: Tidal currents and Kuroshio transport variations in the Tokara Strait estimated from ferryboat ADCP data, J. Geophys. Res., 122, 2120–2142, 2017.

https://doi.org/10.5194/bg-2019-377
Preprint. Discussion started: 7 October 2019

348 **Table 1:** Information on locations and environmental conditions at the stations conducted the gradient enrichment and
349 dilution experiments in the ECS-Kuroshio. Depth: Sampling depth (m) of water samples for each experiment. WT: mean
350 water temperature during the experiments (ºC). $NUTs_o$: nutrients concentrations (µmol L^{-1}) at the beginning of each
351 experiment. CHL_o: Chlorophyll *a* concentration (µgCHL L^{-1}) at the beginning of the experiments. MiZ_o:
352 microzooplankton standing stocks at the beginning of each experiment (µgC L^{-1}). DL: below the detection limit.
353

Station	Location		Date	Year	Depth	WT	$NUTs_o$		CHL_o	MiZ_o
	Longitude	Latitude					NO_3+NO_2	PO_4		
EXP_a										
C02	30°11'N	129°41.0'E	13 Nov	2016	68	26.1	DL	0.02	0.34	0.19
C03	29°50'N	129°08.4'E	13 Nov	2016	75	26.2	DL	0.01	0.41	0.27
F01	29°53'N	129°22.4'E	14 Nov	2016	81	25.1	0.21	0.04	0.35	0.15
G01	29°51'N	129°57.2'E	14 Nov	2016	91	26.1	0.26	0.07	0.44	0.12
K02	29°34'N	128°26.3'E	12 Nov	2017	50	25.6	0.18	DL	0.31	0.23
K05	30°06'N	130°11.9'E	14 Nov	2017	105	24.8	0.57	0.02	0.52	0.79
K08	30°24'N	131°23.6'E	15 Nov	2017	115	25.5	1.82	0.12	0.15	0.34
K11	31°24'N	132°29.2'E	16 Nov	2017	90	25.0	0.16	DL	0.27	0.55
EXP_b										
A05a	30°10'N	129°17.5'E	3 Nov	2017	13	25.5	0.10	0.03	0.23	0.12
A05b	30°10'N	129°17.5'E	7 Nov	2017	95	25.5	DL	DL	0.16	0.15
A05c	30°11'N	129°17.2'E	7 Nov	2017	34	25.3	0.02	0.01	0.24	0.05
A06a	30°00'N	129°15.1'E	3 Nov	2017	12	25.4	DL	0.02	0.16	0.13
A06b	30°00'N	129°15.0'E	7 Nov	2017	110	25.7	1.61	0.11	0.14	0.04
A08a	29°19'N	129°09.4'E	6 Nov	2017	76	25.6	DL	0.02	0.29	0.22
A08b	29°26'N	129°12.4'E	6 Nov	2017	71	25.6	0.03	0.01	0.21	0.17
A09a	29°09'N	129°00.0'E	6 Nov	2017	105	25.6	0.11	0.02	0.20	0.15

https://doi.org/10.5194/bg-2019-377
Preprint. Discussion started: 7 October 2019

Biogeosciences
Discussions
Open Access
EGU

354 Table 2 Phytoplankton growth rate (d^{-1}) derived from the gradient enrichment experiments in the ECS-Kuroshio. Enriched
355 nitrate concentrations (μmol L^{-1}) are shown at the top of each column. A and B: duplicate bottles. Pico: chlorophyll
356 smaller than 2 μm. Nano: chlorophyll between 2 and 11 μm. Micro: chlorophyll larger than 11 μm.

Station	0		0.05		0.15		0.5		0.75		1.5		5	
	A	B	A	B	A	B	A	B	A	B	A	B	A	B
Micro														
C02	-0.108	-0.116	-0.089	-0.082	0.019	-0.073	0.470	0.426	0.422	0.441	0.686	0.798	0.796	0.556
C03	-0.116	-0.118	-0.073	-0.078	-0.004	-0.008	0.453	0.426	0.588	0.706	0.780	0.892	0.862	0.906
F01	0.150	0.159	0.332	0.277	0.282	0.344	0.445	0.495	0.511	0.497	0.490	0.385	0.372	0.467
G01	0.062	0.051	0.135	0.089	0.163	0.108	0.438	0.477	0.795	0.736	0.828	0.969	0.861	0.781
K02	-0.305	-0.282	-0.205	-0.265	-0.113	-0.305	0.264	0.295	0.119	0.097	0.422	0.652	0.831	0.669
K05	-0.147	0.027	0.007	-0.053	0.037	0.084	0.329	0.176	0.263	0.168	0.645	0.716	0.792	0.701
K08	0.348	0.266	0.350	0.315	0.333	0.407	0.361	0.185	0.448	0.416	0.377	0.468	0.403	0.417
K11	-0.062	-0.036	-0.105	-0.092	0.043	-0.081	0.193	0.179	0.514	0.390	0.765	0.730	0.469	0.558
Nano														
C02	-0.479	-0.260	-0.208	-0.409	-0.297	-0.345	-0.050	0.144	0.173	0.151	0.249	0.333	0.330	0.264
C03	-0.275	-0.261	-0.211	-0.257	-0.080	-0.206	0.113	0.031	0.247	0.192	0.363	0.355	0.288	0.256
F01	-0.244	-0.154	-0.286	-0.092	-0.025	0.101	0.182	0.050	0.148	0.039	0.015	0.056	0.104	0.105
G01	-0.304	-0.172	-0.313	-0.189	-0.165	-0.117	-0.063	-0.178	0.100	0.001	0.286	0.325	0.369	0.053
K02	-0.321	-0.149	-0.384	-0.152	0.022	0.035	0.223	0.251	-0.027	-0.135	0.433	0.229	0.559	0.523
K05	-0.389	-0.318	-0.680	-0.546	-0.267	-0.394	-0.484	-0.248	-0.407	-0.458	0.053	-0.034	0.102	0.196
K08	0.353	0.244	0.508	0.472	0.455	0.436	0.406	0.397	0.473	0.369	0.408	0.546	0.380	0.384
K11	-0.138	-0.088	-0.257	-0.243	-0.134	-0.293	0.073	0.026	0.175	0.201	0.296	0.312	0.434	0.501
Pico														
C02	-0.383	-0.188	-0.186	-0.199	-0.119	-0.162	0.188	0.143	0.162	0.241	0.257	0.291	0.377	0.205
C03	-0.202	-0.258	-0.259	-0.282	-0.143	-0.160	0.017	-0.019	0.148	0.191	0.194	0.248	0.230	0.300
F01	-0.071	-0.091	-0.054	-0.032	0.050	0.129	0.205	0.144	0.216	0.141	0.170	0.134	0.031	0.172
G01	0.019	-0.061	0.051	-0.032	0.019	0.008	0.156	0.162	0.323	0.188	0.338	0.308	0.344	0.366
K02	-0.245	-0.253	-0.257	-0.275	-0.243	-0.230	-0.046	0.010	-0.067	-0.101	0.065	-0.030	0.203	0.089
K05	-0.087	0.031	0.014	-0.027	0.103	0.157	0.057	0.261	0.130	0.339	0.316	0.255	0.368	0.404
K08	0.032	0.055	-0.013	0.228	0.262	0.201	0.240	0.069	0.262	0.281	0.177	0.284	0.222	0.327
K11	-0.197	-0.216	-0.194	-0.146	-0.046	-0.071	-0.005	0.033	0.163	0.076	0.236	0.049	0.092	0.179

357

Table 3 Parameters derived from the dilution experiments in the ECS-Kuroshio. g_{max}: maximum growth rate (d^{-1}). m: mortality rate by microzooplankton grazing (d^{-1}). g_o: net growth rate measured in the non-enriched and non-diluted bottles (d^{-1}). g_{en}: net growth rate measured in the enriched and non-diluted bottles (d^{-1}). r^2: coefficient of determination defined from the linear regression of the apparent growth rate of total chlorophyll *a* concentrations against dilution factors. p: p-value. Pico: chlorophyll smaller than 2 µm. Nano: chlorophyll between 2 and 11 µm. Micro: chlorophyll larger than 11 µm. Total: total chlorophyll from pico- to micro.

Station	Pico				Nano				Micro				Total					
	g_{max}	m	g_o	g_{en}	g_{max}	m	g_o	g_{en}	g_{max}	m	g_o	g_{en}	g_{max}	m	g_o	g_{en}	r^2	p
A05a	0.283	0.887	0.415	0.681	1.181	1.345	-0.267	0.181	0.913	0.962	0.059	0.045	1.059	0.619	0.199	0.492	0.757	<0.01
A05b	0.931	1.106	-0.109	0.279	1.354	1.050	-0.505	-0.239	0.477	0.583	-0.030	0.107	1.073	1.051	-0.232	0.113	0.901	<0.01
A05c	0.501	0.647	-0.025	0.190	1.298	1.192	-0.183	-0.066	0.313	0.500	-0.269	0.201	0.828	0.752	-0.074	0.122	0.875	<0.01
A06a	0.179	0.814	0.440	0.646	0.865	1.270	0.247	0.341	0.232	0.597	-0.315	0.339	0.941	0.381	0.347	0.550	0.541	<0.01
A06b	0.648	-0.398	-0.869	-1.020	0.947	0.247	-0.789	-0.629	-0.118	-0.037	-0.038	0.065	-0.052	0.711	-0.735	-0.714	0.750	<0.01
A08a	0.434	0.458	-0.097	0.035	1.448	1.289	-0.072	-0.150	0.401	0.564	-0.537	0.181	0.765	0.775	-0.113	0.009	0.856	<0.01
A08b	0.370	0.846	-0.040	0.509	0.652	1.068	-0.259	0.430	0.553	1.122	-0.620	0.529	0.937	0.471	-0.123	0.488	0.693	<0.01
A09a	0.488	0.417	-0.399	-0.026	0.894	0.734	-0.182	-0.082	0.353	0.022	-0.474	-0.235	0.526	0.640	-0.324	-0.052	0.760	<0.01

https://doi.org/10.5194/bg-2019-377
Preprint. Discussion started: 7 October 2019

Biogeosciences Discussions Open Access EGU

364 **Table 4** Parameters derived from relationship of phytoplankton growth rates against logarithmically transformed
365 concentrations of enriched nitrate. Slope: sensitivity of phytoplankton growth rate to logarithmically transformed
366 concentrations of enriched nitrate. Intercept: growth potential at the low nitrate concentration. r^2: coefficient of
367 determination defined from the linear regression of growth rate of size-fractionated chlorophyll *a* concentrations against
368 logarithmically transformed concentrations of enriched nitrate enrichment. Pico: chlorophyll smaller than 2 µm. Nano:
369 chlorophyll between 2 and 11 µm. Micro: chlorophyll larger than 11 µm.
370
371

Station	Pico			Nano			Micro		
	Slope	Intercept	r^2	Slope	Intercept	r^2	Slope	Intercept	r^2
C02	0.281	0.178	0.848	0.370	0.131	0.831	0.458	0.492	0.846
C03	0.295	0.121	0.922	0.308	0.177	0.830	0.560	0.611	0.914
F01	0.074	0.129	0.317	0.120	0.067	0.420	0.077	0.430	0.368
G01	0.203	0.243	0.866	0.272	0.085	0.688	0.448	0.657	0.817
K02	0.213	-0.014	0.883	0.364	0.233	0.726	0.531	0.353	0.872
K05	0.188	0.251	0.772	0.355	-0.165	0.729	0.419	0.439	0.843
K08	0.070	0.231	0.242	-0.038	0.426	0.213	0.045	0.386	0.162
K11	0.167	0.077	0.750	0.394	0.201	0.943	0.403	0.409	0.744

https://doi.org/10.5194/bg-2019-377
Preprint. Discussion started: 7 October 2019

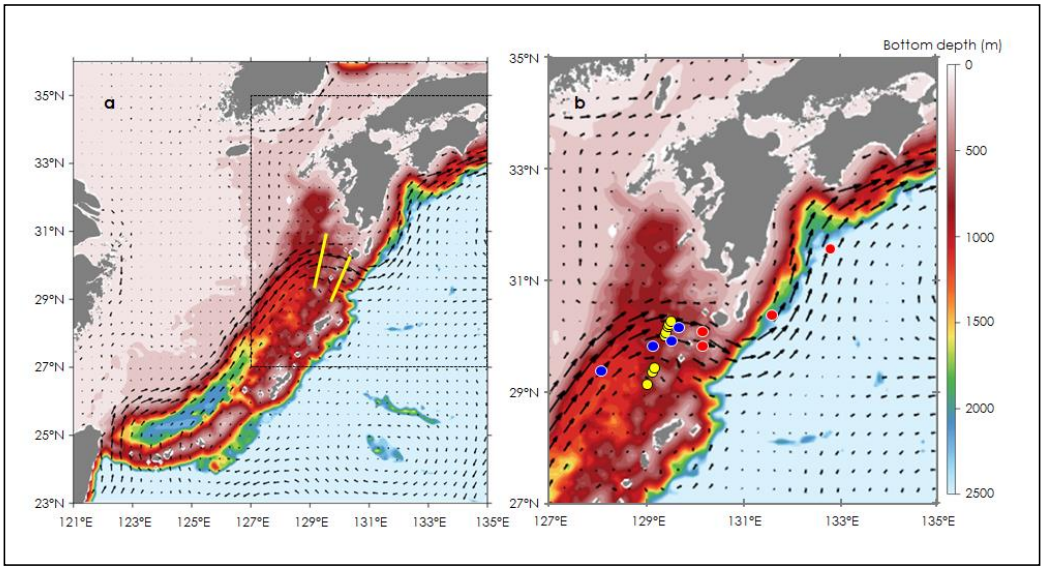

Figure 1 Locations for oceanographic observations and onboard experiments in the Kuroshio Current of the East China Sea (ECS-Kuroshio). **(a)** Oceanographic observations by Deep SUNA V2 and TurboMAP-L (yellow lines). **(b)** Onboard experiments for phytoplankton and microzooplankton growth (EXP_a: red and blue circles) and for microzooplankton grazing (EXP_b: yellow circles). EXP_a are conducted in the upstream (blue circles) and downstream Kuroshio (red circles) in the Tokara Strait. Current directions and velocities (arrows) are shown as monthly means during November 2016. Bottom depth (m) is indicated as colored contours.

https://doi.org/10.5194/bg-2019-377
Preprint. Discussion started: 7 October 2019

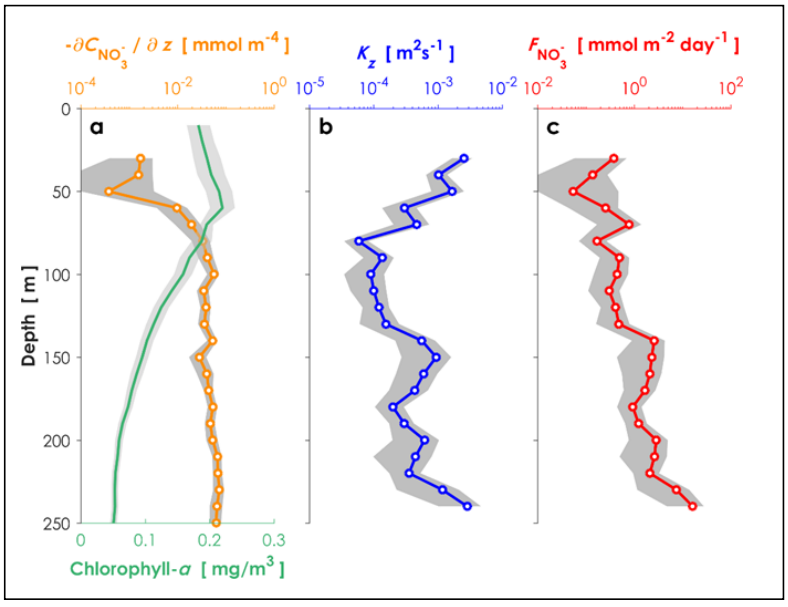

379

380 **Figure 2** Vertical profiles of environmental conditions in the Kuroshio Current. **(a)** Nitrate concentration (orange) and
381 chlorophyll *a* concentrations (green) measured with a nitrate sensor (Deep SUNA V2) attached to an SBE-9plus CTD
382 system. **(b)** Turbulent diffusivity measured with a TurboMAP-L (blue). (**c**) Calculated turbulent nitrate fluxes (red) in the
383 ECS-Kuroshio. The shaded areas are the 95 percent confidence intervals obtained by a bootstrap process.

https://doi.org/10.5194/bg-2019-377
Preprint. Discussion started: 7 October 2019

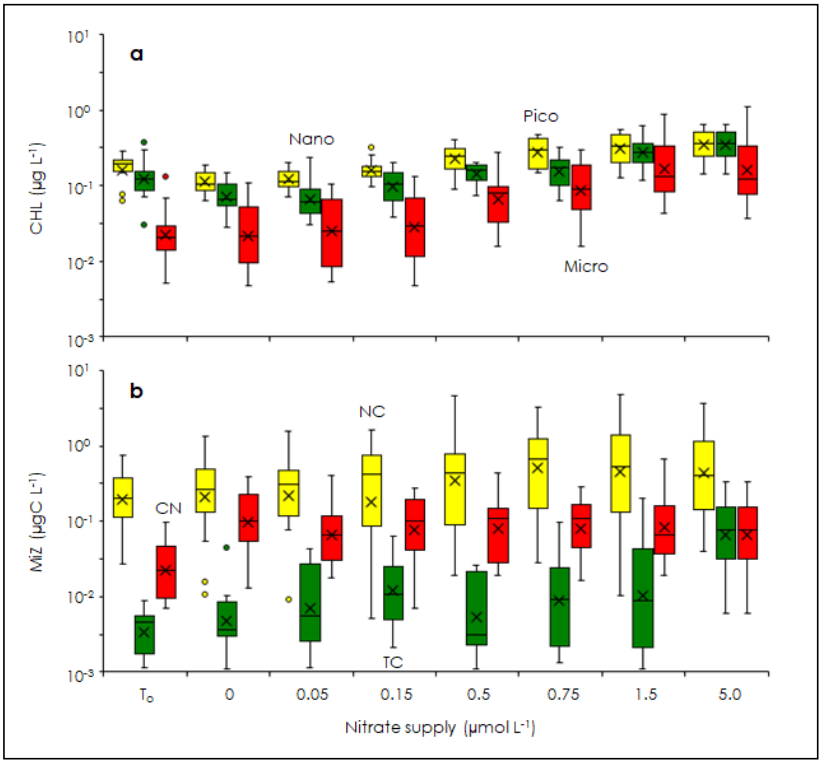

Figure 3 Changes in phytoplankton and microzooplankton standing stocks during the gradient enrichment experiments. **(a)** Size-fractionated chlorophyll *a* concentrations (CHL). **(b)** Microzooplankton standing stocks (MiZ). T_o: at the beginning of the gradient enrichment experiments. 0: no enrichment. 0.05 to 5.0 µmol L^{-1}: enrichment. Box-and-whisker diagram at each nitrate concentrations was compiled with the results conducted at the 8 stations. Box represents first (bottom), second (bar) and third (top) quartiles, and cross marks are the average values. Whiskers indicate minimum and maximum values, and circles are outliers. Pico: chlorophyll smaller than 2 µm (yellow). Nano: chlorophyll between 2 and 11 µm (green). Micro: chlorophyll larger than 11 µm (red). NC: naked ciliates (yellow). TC: tintinnid ciliates (green). CN: copepod nauplii (red).

https://doi.org/10.5194/bg-2019-377
Preprint. Discussion started: 7 October 2019

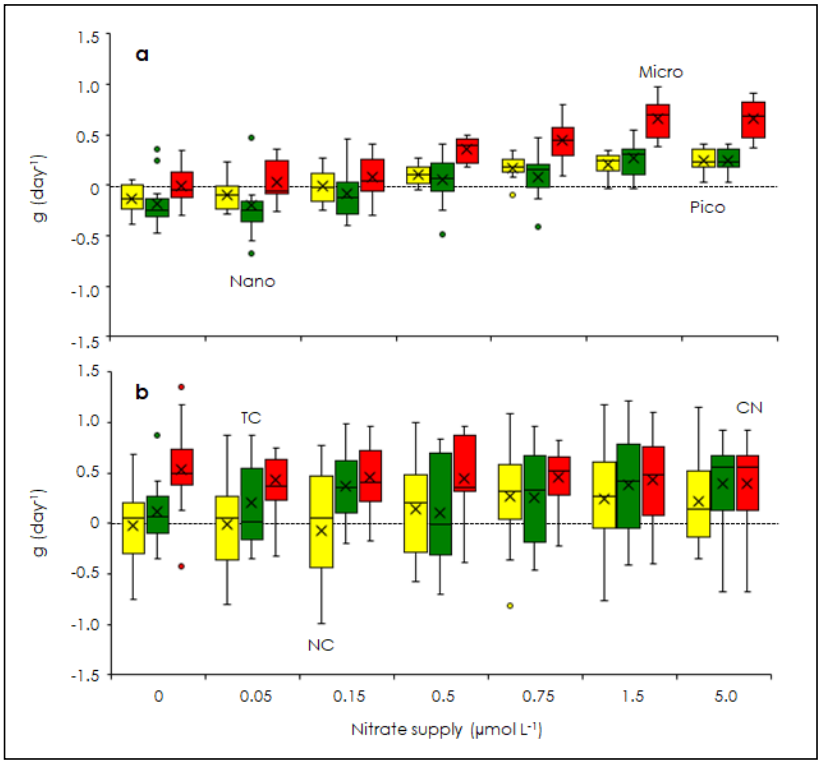

Figure 4 Changes in phytoplankton and microzooplankton growth rates in response to nitrate enrichments in the gradient enrichment experiments. **(a)** Growth rates (g: d^{-1}) of size-fractionated chlorophyll. **(b)** Microzooplankton growth rates (g: d^{-1}). 0: no enrichment. 0.05 to 5.0 µmol L^{-1}: enrichment. Box-and-whisker diagram at each nitrate concentration is based on the results conducted at the eight stations. The symbols have the same meaning as in Figure 3.

https://doi.org/10.5194/bg-2019-377
Preprint. Discussion started: 7 October 2019

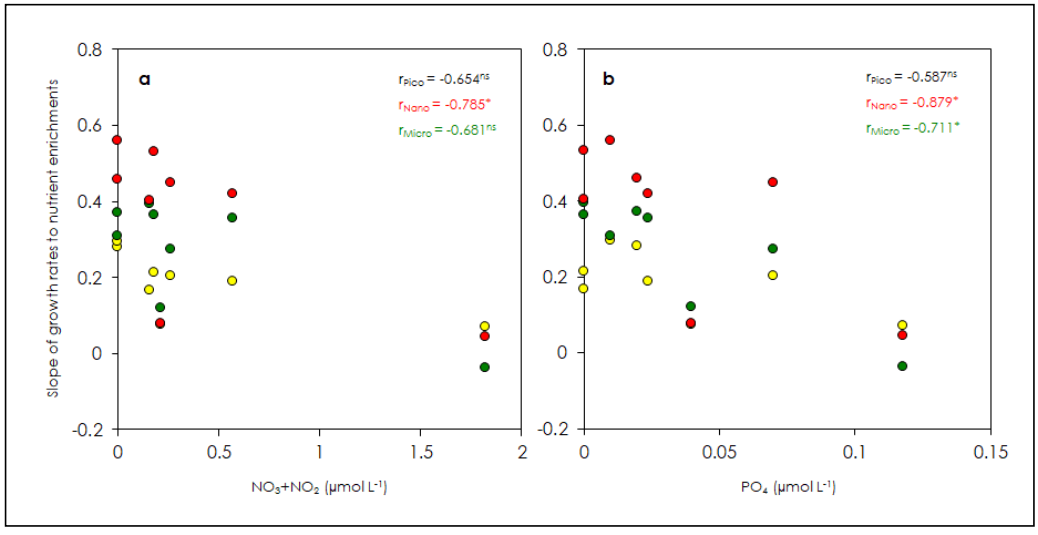

Figure 5 Correlation of the regression slopes of phytoplankton growth rates to logarithmically transformed nutrients concentrations at the beginning of the gradient enrichment experiments. **(a)** Regression slopes of the size-fractionated phytoplankton growth versus the logarithmically transformed concentrations of nitrate (NO_3) plus nitrite (NO_2). **(b)** Regression slopes of the size-fractionated phytoplankton growth versus the logarithmically transformed concentrations of phosphate concentrations. r: Pearson correlation coefficient. Pico: chlorophyll smaller than 2 µm. Nano: chlorophyll between 2 and 11 µm. Micro: chlorophyll larger than 11 µm. *: p<0.05. ns: no significant.

https://doi.org/10.5194/bg-2019-377
Preprint. Discussion started: 7 October 2019

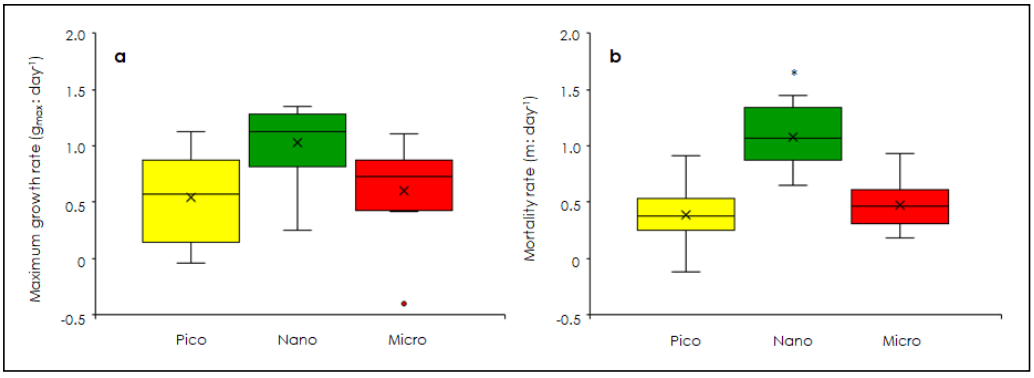

Figure 6 Comparisons of phytoplankton growth and mortality rates among the three size-fractionated chlorophyll. **(a)** Maximum growth rates (g_{max}). **(b)** Mortality rates by mirozooplankton grazing. Box-and-whisker diagram at each nitrate concentrations was compiled with the results conducted at the 8 stations. Box represents first (bottom), second (bar) and third (top) quartiles, and cross marks are the average values. Whiskers indicate minimum and maximum values, and circles are outliers. Asterisk means significant difference among the three size-fractions (ANOVA+Tukey, $p<0.05$). Pico: chlorophyll smaller than 2 µm. Nano: chlorophyll between 2 and 11 µm. Micro: chlorophyll larger than 11 µm.

https://doi.org/10.5194/bg-2019-377
Preprint. Discussion started: 7 October 2019

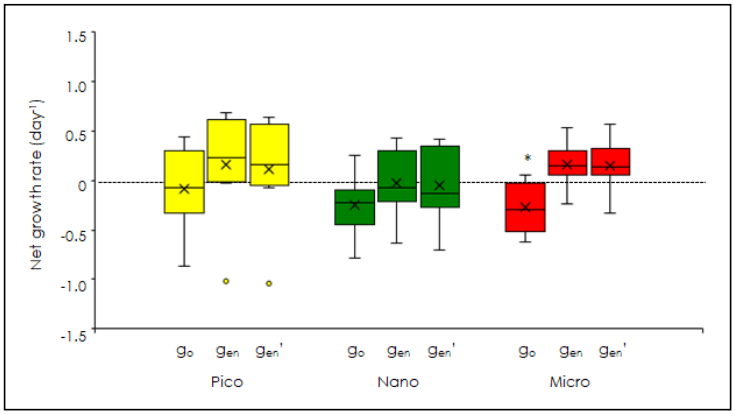

412

413 **Figure 7** Comparisons of phytoplankton net growth among the three different methods. g_o: Observed net growth rates
414 without enrichment in the non-diluted bottles. g_{en}: Observed net growth rates with enrichment in the non-diluted bottles.
415 g_{en}': Estimated net growth rates subtracting the mortality rates (m) from the maximum growth rates (g_{max}). Box-and-
416 whisker diagram at each nitrate concentrations was compiled with the results conducted at the 8 stations. Asterisk means
417 significant difference between g_o and g_{en} (Welch's *t*-test, $p<0.05$). The symbols have the same meaning as in Figure 6.